Acta Math. Univ. Comenianae
Vol. LXVII, 1(1998), pp. 115–136

ADAPTIVE FINITE VOLUME DISCRETIZATION OF DENSITY DRIVEN FLOWS IN POROUS MEDIA

P. KNABNER, C. TAPP AND K. THIELE

1. Introduction

The present paper deals with the mathematical treatment of the system of partial differential equations, arising from the modeling of density driven flow in porous media. A detailed description of the model is given by e.g. Leijnse [**13**]. The system is of a highly nonlinear and parabolic-elliptic type.

For the discretization of the problem, we use Finite Volume and/or Mixed Finite Element Methods. For typical field applications in conjunction with safety studies for underground waste repositories, simulations are required for large domains Ω and a long time interval $(0, T)$. This requirement leads to relatively large mesh and time step sizes because of computational limitation. This makes it necessary to consider discretization methods, where the solution fulfils proper physical properties. For the chosen methods local conservation laws are fulfiled. Moreover we use an error indicator to create an adaptive grid aiming at an optimal use of computer power. By discretising the Darcy velocity artificial numerical velocities can appear (cf. [**14**]). To prevent this we use a consistent approximation of the velocity which is based on the ideas of [**12**].

It is well known in literature (cf. [**10**]) that for discontinuous and anisotropic permeability the finite volume discretization causes some problems, because only concentration and pressure are the primary variables and the velocity field has to be approximated by a post-processing step. A mixed element discretization, however, approximates the velocity directly and may gain advantages in such a situation.

To stabilize the numerical solution w.r.t. non-physical oscillations, we use some upwind techniques. The most common method is the "full upwind". We also use other upwind techniques, where the algorithm exhibits less artificial diffusion. These techniques are described in the companion paper [**11**].

It should be mentioned that the theoretical analysis of the method is far from complete. At the moment there are a lot of assumptions, conjectures, etc., which

Received November 15, 1997.
1980 *Mathematics Subject Classification* (1991 *Revision*). Primary 65M60, 65M15.

can either not be proved rigorously, or not be proved in general that the practical experiences would indicate they hold. Nevertheless the numerical experiments show, that with the finite volume discretization, the upwind and the adaptive grid control based on the error indicators, we have a powerful tool for solving density driven flow problems.

The paper is structured in the following way. In the second Section, we introduce the mathematical model of density driven flow in porous media. The discretization in space is explained in Section 3 and 4. First we consider the discretization of the transport equation in Section 3. For the flow equation, we compare different types of discretizations in Section 4. An a posteriori error indicator for the error in the finite volume discretization is introduced in Section 5. In the last Section we give some explanations of the adaptive algorithm and show numerical results for the introduced types of discretizations and for the adaptive algorithm.

We consider a domain $\Omega \in \mathbb{R}^n$, $n = 1, 2$ for any open subset $\omega \subset \Omega$, $L^q(\omega)$ and $W_q^l(\omega)$ with $1 \leq q \leq \infty$, $l \in \mathbb{N}$ denote the standard real Lebesgue- and Sobolev spaces endowed with the norms $\|\cdot\|_{0,p,\omega}$ and $\|\cdot\|_{l,p,\omega}$, respectively. By $(\cdot,\cdot)$ the inner product in $L^2(\Omega)$ or $L^2(\Omega) \times L^2(\Omega)$ is denoted. If $\omega = \Omega$ the subscript ω is omitted. Moreover, we set $H^l(\Omega) := W_2^l(\Omega)$ and $H_0^l(\Omega)$ is the space of all the functions in $H^l(\Omega)$ vanishing on the boundary Γ of Ω in the usual sense of traces. The solution space is $\mathbf{V}_0 := V_0 \times V_0$ with $V_0 \subset W_q^l(\omega)$, for some $q > 1$.

2. Mathematical Model

Given a bounded domain $\Omega \subset \mathbb{R}^d$, $d = 2$ or $d = 3$, with polyhedral Lipschitzian boundary and an interval $(0, T)$, $T > 0$, the following nonlinear system of partial differential equations is considered:

$$\Phi \frac{\partial \rho c}{\partial t} + \nabla \cdot (\mathbf{q}\rho c - \rho D \nabla c) = Q\,, \tag{1}$$

$$\Phi \frac{\partial \rho}{\partial t} + \nabla \cdot (\rho \mathbf{q}) = \tilde{Q}\,, \tag{2}$$

where the so-called **Darcy velocity q** is given by

$$\mathbf{q} = -\mu^{-1} K (\nabla p - \rho \mathbf{g})\,. \tag{3}$$

These equations arise from the modelling of the transport of dissolved salt in flowing groundwater. The unknown functions are the mass fraction (concentration) $c = c(x,t)$ and the pressure $p = p(x,t)$. A detailed discussion of the model can be found in [**13**]. The equation (1) is called transport equation and equation (2) flow equation. In particular we got the permeability tensor $K\colon \Omega \to \mathbb{R}^{d\times d}$, the porosity $\phi\colon \Omega \to (0,1)$, the source and sink terms $Q, \tilde{Q}\colon (0,T) \times \Omega \to \mathbb{R}$ and the

gravity $\mathbf{g} \in \mathbb{R}^d$. In general, the viscosity and the density $\mu, \rho\colon \mathbb{R} \to \mathbb{R}$ are nonlinear functions of c, i.e. $\mu = \mu(c)$, $\rho = \rho(c)$, with $\mu, \rho > 0$, and the dispersion-diffusion tensor $D\colon \mathbb{R}^d \to \mathbb{R}^{d\times d}$ is nonlinearly depending on $\mathbf{q}$.

The system is completed by the initial condition $c(0) = c_0$ and by boundary conditions for the unknowns $\binom{c}{p}$, where the latter are of different types at different parts of the boundary of Ω.

To the authors' knowledge, up to now no theory of existence, uniqueness, long-time behaviour etc. of solution(s) of (1)–(3) is present. Therefore we have to make a corresponding assumption:

> There exist numbers $T > 0$ and $q > 1$ such that problem (1)–(3) possesses a unique solution $\binom{c(t)}{p(t)} \in \mathbf{V}_0 = V_0 \times V_0 \subset W_q^1(\Omega) \times W_q^1(\Omega),\ t \in (0, T)$.

I.e., this is the characterizing property of the space $\mathbf{V}_0$.

3. Finite Volume Discretization of the Transport Equation

We restrict the explanation of the discretization to the 2D case. The 3D case follows analogously only by replacing triangle by tetrahedron, edge by face etc. Starting from an admissible partition $\mathcal{T}$ of Ω consisting of triangles or quadrilaterals T^e, $e = 1, \dots, M$, we define finite-dimensional spaces $V_h \subset V_0$ such that the restriction of their elements to a triangle or a quadrilaterals is a linear or bilinear function, respectively. By N we denote the number of all vertices of the partition, whereas I is the number of interior vertices.

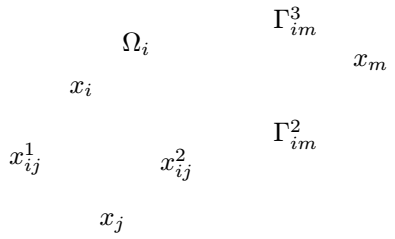

Figure 1. Vertex-centered finite volume.

Following the so called vertex-centered finite volume methods, we construct a dual mesh of **control volumes** Ω_i, $i = 1, \dots, N$, by means of Donald diagrams. Within an element T^e, the barycenter is connected with the midpoints of the element edges between the nodes x_i and x_j by a straight-line segment Γ_{ij}^e, the midpoint of which is denoted by x_{ij}^e. Here we have $e \in \Lambda_{ij}$, where Λ_{ij} denotes the set of indices e of all elements which contain the nodes x_i and x_j. So we get, for any vertex x_i, a closed polygon containing it. This polygon forms the boundary

of Ω_i. The numerical procedure calculates the unknowns at the vertex x_i, which is the center of the finite volume Ω_i.

To derive the discretization, the equation (1) is integrated over the finite volumes Ω_i, $i = 1, \dots, N$, and then Green's formula is applied. The equations become

$$\int_{\Omega_i} \phi \frac{\partial \rho c}{\partial t}\, dx + \int_{\partial\Omega_i} \rho c \mathbf{n} \cdot \mathbf{q}\, ds - \int_{\partial\Omega_i} \rho \mathbf{n} \cdot D\, \nabla c\, ds = \int_{\Omega_i} Q\, dx.$$

The arising integrals over Ω_i and along the boundary $\partial\Omega_i$ are approximated. In particular, for the first one we use the quadrature rule

$$\int_{\Omega_i} u\, dx \approx u(x_i)|\Omega_i|, \tag{4}$$

where $|\Omega_i|$ is the area of the subdomain Ω_i.

The boundary integrals we approximate by

$$\int_{\partial\Omega_i} \rho c \mathbf{n}\cdot\mathbf{q}\, ds - \int_{\partial\Omega_i} \rho \mathbf{n}\cdot D\cdot\nabla c\, ds \approx \sum_{j,e} |\Gamma_{ij}^e| \mathbf{n}_{ij}^e \cdot \left(\frac{1}{2} \rho_{ij}^e \mathbf{q}_{ij}^e (c_i + c_j) - \mathcal{K}_{ij}^e \rho_{ij}^e D_{ij}^e \nabla c_{ij}^e \right)$$

where $|\Gamma_{ij}^e|$ is the length of the boundary segment Γ_{ij}^e. The outer normal w.r.t. Ω_i on Γ_{ij}^e is called $\mathbf{n}_{ij}^e$. For the indices we got $j \in \Lambda_i$ where j is the index of all neighbour nodes x_j to x_i; and $e \in \Lambda_{ij}$. To stabilize the numerical solution w.r.t. non-physical oscillations, we use some upwind techniques which are described by Frolkovič [**11**]. With $\mathcal{K}$ we denote a scalar function, dependent on the local Peclet number, with $\mathcal{K}(0) = 1$ and $\mathcal{K} \geq 1$. $\mathcal{K}$ describes the different types of upwind. For $\mathcal{K} \equiv 1$ we have no-upwind, that means the integral is approximated by a standard quadrature rule. In [**11**] also the use of $\frac{1}{2}(c_i + c_j)$ instead of c_{ij}^e in the approximation of the convective term will be explained.

For the sake of a short notation, we write $c_i := c_h(x_i)$, $p_i := p_h(x_i)$, etc. and $c_{ij}^e := c_h(x_{ij}^e)$, $p_{ij}^e := p_h(x_{ij}^e)$ etc. Composite functions are abbreviated by $\rho_h := \rho(c_h)$ and $\rho_h(x) := \rho(c_h(x))$, $\rho_i = \rho(c_i)$ and $\rho_{ij}^e = \rho(c_{ij}^e)$ etc.

So we arrive at the following discrete equation:

$$|\Omega_i|\phi_i \partial_t(\rho_i c_i) + \sum_{j,e} |\Gamma_{ij}^e| \mathbf{n}_{ij}^e \cdot \big(\frac{1}{2} \rho_{ij}^e \mathbf{q}_{ij}^e (c_i + c_j) - \mathcal{K}_{ij}^e \rho_{ij}^e D_{ij}^e \nabla c_{ij}^e \big) = |\Omega_i| Q_i$$

where $\mathbf{q}$ is defined as in (3).

4. Discretization of the Flow Equation

We use different kinds of discretizations for the flow equation.

4.1 Finite Volume Discretization

The flow equation can be treated in the same way as the transport equation in the previous section. So we get for the semi-discrete problem:

Find $(c_h(t), p_h(t)) \in \mathbf{V}_h := V_h \times V_h$, such that for all $t \in (0,T)$ holds:

$$|\Omega_i|\phi_i \partial_t \rho_i + \sum_{j,e} |\Gamma_{ij}^e| \mathbf{n}_{ij}^e \cdot \rho_{ij}^e \mathbf{q}_{ij}^e = |\Omega_i| \tilde{Q}_i \tag{5}$$

$$|\Omega_i|\phi_i \partial_t (\rho_i c_i) + \sum_{j,e} |\Gamma_{ij}^e| \mathbf{n}_{ij}^e \cdot \left(\frac{1}{2} \rho_{ij}^e \mathbf{q}_{ij}^e (c_i + c_j) - \mathcal{K}_{ij}^e \rho_{ij}^e D_{ij}^e \nabla c_{ij}^e \right) = |\Omega_i| Q_i \tag{6}$$

with suitable initial and boundary condition corresponding to the continuous problem. The Darcy velocity is defined in discrete form as in (3).

We make the following assumption about the existence and uniqueness of a solution:

> There exist $T > 0$ such that problem (5)–(6)possesses a unique solution $\binom{c_h(t)}{p_h(t)} \in \mathbf{V}_h,\ t \in (0,T)$.

The arising system of ordinary differential equations is solved e.g. by the implicit Euler method or a higher order time discretization.

For reason of simplicity we further restrict ourselves to the case $Q, \tilde{Q} \equiv 0$, Dirichlet boundary conditions and triangular elements.

4.2 Mixed Finite Element Discretization

In the previous section a discretization of the flow equation with the unknowns (c,p) is formulated. In the mixed finite element method, the Darcy's law and flow equation are approximated individually and we get additionally the Darcy velocity $\mathbf{q}$ as an unknown function.

Introducing the Hilbert space

$$H(\mathrm{div}\,;\Omega) = \left\{ \boldsymbol{\chi} \in \left(L^2(\Omega)\right)^2 \mid \nabla \cdot \boldsymbol{\chi} \in L^2(\Omega) \right\}$$

the mixed formulation of (2)–(3) is given as:

Find $(\mathbf{q}, p) \in H(\mathrm{div}\,;\Omega) \times L^2(\Omega)$ such that

$$\begin{aligned} a(\mathbf{q}, \boldsymbol{\chi}) - b(p, \boldsymbol{\chi}) &= (\rho \mathbf{g}, \boldsymbol{\chi}) - \langle p_D, \boldsymbol{\chi} \cdot \mathbf{n} \rangle \qquad && \forall \boldsymbol{\chi} \in H(\mathrm{div}\,;\Omega) \\ b(\varphi, \rho \mathbf{q}) &= -(\phi \frac{\partial \rho}{\partial t}, \varphi) + (\tilde{Q}, \varphi) \qquad && \forall \varphi \in L^2(\Omega) \end{aligned}$$

where the bilinear forms are defined as

$$a : \begin{cases} H(\mathrm{div}\,;\Omega) \times H(\mathrm{div}\,;\Omega) \longrightarrow \mathbb{R} \\ (\mathbf{q}_1, \mathbf{q}_2) \longmapsto \int_\Omega K^{-1} \mu \mathbf{q}_1 \cdot \mathbf{q}_2 \, dx \end{cases}$$

$$b : \begin{cases} L^2(\Omega) \times H(\mathrm{div}\,;\Omega) \longrightarrow \mathbb{R} \\ (v, \mathbf{q}) \longmapsto \int_\Omega \nabla \cdot \mathbf{q} v \, dx \end{cases}$$

$(\cdot,\cdot)$ and $\langle\cdot,\cdot\rangle$ denote the usual inner products in $(L(\Omega)^2)^2$, respectively $L^2(\Omega)$ and $L^2(\partial\Omega)$.

At the moment we consider Dirichlet boundary condition, where p_D is the prescribed pressure p on the boundary.

Using the triangulation of the previous section, the following notation is introduced: The edges of an element $T \in \mathcal{T}$ are referred to as e_i, $1 \le i \le 3$. We denote by $\mathcal{E}$ the set of edges of $\mathcal{T}$ and by

$$\mathcal{E}^0 = \mathcal{E} \cap \Omega,$$
$$\mathcal{E}^\partial = \mathcal{E} \cap \partial\Omega$$

the subsets of interior and boundary edges, respectively.

For $D \subseteq \Omega$ we denote the space of polynomials of degree $\le k$ by $P_k(D)$.

An approximation V_h of $H(\mathrm{div}\,,\Omega)$ is given by the Raviart-Thomas space $RT_0(\Omega,\mathcal{T})$:

$$RT_0(\Omega,\mathcal{T}) := \{\boldsymbol{\chi} \in H(\mathrm{div}\,,\Omega) | \boldsymbol{\chi}|_T \in RT_0(T), \quad T \in \mathcal{T}\}\,,$$

where $RT_0(T)$ stands for the lowest order Raviart-Thomas element

$$RT_0(T) := (P_0(T))^2 + \mathbf{x} \cdot P_0(T).$$

Every $\boldsymbol{\chi} \in RT_0(T)$ is uniquely determined by the normal fluxes $\mathbf{n} \cdot \boldsymbol{\chi}$ on the edges e_i, $1 \le i \le 3$, where $\mathbf{n}$ denotes the outer normal w.r.t. the element T.

As a finite dimensional subspace $M_h(\mathcal{T}) \subset L^2(\Omega)$ we take the space of piecewise constant functions:

$$M_h(\mathcal{T}) := \left\{\varphi \in L^2(\Omega) \mid \varphi\,|_T \in P_0(T), T \in \mathcal{T}\right\}.$$

Simple calculation shows

$$\mathrm{div}\ V_h = M_h(\mathcal{T}).$$

The standard mixed discretization reads as follows:

Find $(\mathbf{q}_h, p_h) \in V_h \times M_h(\mathcal{T})$ such that

$$\begin{aligned} a(\mathbf{q}_h,\boldsymbol{\chi}_h) - b(p_h,\boldsymbol{\chi}_h) &= (\rho_h \mathbf{g},\boldsymbol{\chi}_h) - \langle p_D, \boldsymbol{\chi}_h \cdot \mathbf{n}\rangle \qquad \forall \boldsymbol{\chi}_h \in V_h \\ b(\varphi_h,\rho_h\mathbf{q}_h) &= -\big(\phi\frac{\partial \rho_h}{\partial t},\varphi_h\big) + (\tilde{Q},\varphi_h) \qquad \forall \varphi_h \in M_h(T). \end{aligned} \tag{7}$$

This leads to an indefinite saddle point problem after linearization. To overcome this difficulty, we use the technique of hybridisation. For more information see [**3**], [**9**].

Relaxing the continuity condition of the ansatz functions in $RT_0(\Omega, \mathcal{T})$ we use the non-conforming space

$$\hat{V_h} = R_0^{-1}(\Omega, \mathcal{T}) := \left\{ \boldsymbol{\chi} \in (L^2(\Omega))^2 \mid \boldsymbol{\chi}|_T \in RT_0(T), T \in \mathcal{T} \right\}.$$

The continuity of the normal flux over element boundaries is guaranteed by Lagrange multipliers from $M_h^0(\mathcal{E})$, where

$$M_h(\mathcal{E}) := \left\{ \mu_h \in L^2(\mathcal{E}) \mid \mu_h|_e \in P_0(e), e \in \mathcal{E} \right\}$$

and

$$M_h^0(\mathcal{E}) := \{ \mu_h \in M_h(\mathcal{E}) \mid \mu_h|_e = 0, e \subset \partial\Omega \}.$$

Furthermore define

$$M_h^D(\mathcal{E}) := \{ \mu_h \in M_h(\mathcal{E}) \mid \mu_h|_e = p_D, e \subset \partial\Omega \}.$$

Then the mixed hybrid discretization reads as:

Find $(\mathbf{q}_h^*, p_h^*, \lambda_h) \in \hat{V_h} \times M_h(\mathcal{T}) \times M_h^D(\mathcal{E})$ such that

$$\begin{aligned} \hat{a}(\mathbf{q}_h^*, \boldsymbol{\chi}_h) - \hat{b}(p_h^*, \boldsymbol{\chi}_h) + c(\lambda_h, \boldsymbol{\chi}_h) &= (\rho_h \mathbf{g}, \boldsymbol{\chi}_h) - \langle p_D, \boldsymbol{\chi}_h \cdot \mathbf{n} \rangle && \forall \boldsymbol{\chi}_h \in \hat{V_h} \\ \hat{b}(\varphi_h, \rho_h \mathbf{q}_h^*) &= -(\phi \frac{\partial \rho_h}{\partial t}, \varphi_h) + (\tilde{Q}, \varphi_h) && \forall \varphi_h \in M_h(\mathcal{T}) \\ c(\mu_h, \mathbf{q}_h^*) &= 0 && \forall \mu_h \in M_h^0(\mathcal{E}) \end{aligned} \tag{8}$$

where

$$\hat{a} : \begin{cases} \hat{V_h} \times \hat{V_h} \longrightarrow \mathbb{R} \\ (\mathbf{q}_1, \mathbf{q}_2) \longmapsto \sum_{T \in \mathcal{T}} \int_T K^{-1} \mu \mathbf{q}_1 \cdot \mathbf{q}_2 \, dx \end{cases} \tag{9}$$

$$\hat{b} : \begin{cases} M_h(\mathcal{T}) \times \hat{V_h} \longrightarrow \mathbb{R} \\ \hat{b}(v, \mathbf{q}) \longmapsto \sum_{T \in \mathcal{T}} \int_T \nabla \cdot \mathbf{q} v \, dx \end{cases} \tag{10}$$

$$c : \begin{cases} M_h(\mathcal{E}) \times \hat{V_h} \longrightarrow \mathbb{R} \\ c(v, \mathbf{q}) \longmapsto \sum_{T \in \mathcal{T}} \int_{\partial T} v \mathbf{q} \cdot \mathbf{n} \, ds \end{cases} \tag{11}$$

For a solution $(\mathbf{q}_h^*, p_h^*, \lambda_h)$ of (8), the last equation in (8) implies $\mathbf{q}_h^* \in RT_0$. If $(\mathbf{q}_h, p_h) \in V_h \times M_h(T)$ solves (7), the last equation in (8) is automatically fulfilled. That means we drop the * in (8) and have

$$\begin{aligned} \mathbf{q}_h^* &= \mathbf{q}_h, \\ p_h^* &= p_h. \end{aligned}$$

Static condensation

Now we eliminate the unknown flux in (8). For every triangle $T \in \mathcal{T}$ there exist 3 test functions $\boldsymbol{\chi}_i \in \hat{V}_h$ with

$$\text{supp}\,(\boldsymbol{\chi}_i) \subseteq T.$$

Consider the first equation in (8) on element level. One gets (ignoring boundary terms)

$$A \begin{pmatrix} q_1 \\ q_2 \\ q_3 \end{pmatrix} = \begin{pmatrix} b_1 \\ b_2 \\ b_3 \end{pmatrix} - \begin{pmatrix} c_1 \\ c_2 \\ c_3 \end{pmatrix} + \begin{pmatrix} d_1 \\ d_2 \\ d_3 \end{pmatrix},$$

where A is a 3×3 matrix with entries of the form

$$(A)_{ij} = \hat{a}(\boldsymbol{\chi}_i, \boldsymbol{\chi}_j).$$

We define b_i, c_i, d_i as follows:

$$\begin{aligned} b_i &= \hat{b}(p_h, \boldsymbol{\chi}_i), \\ c_i &= \hat{c}(\lambda_h, \boldsymbol{\chi}_i), \\ d_i &= (\rho_h \mathbf{g}, \boldsymbol{\chi}_i). \end{aligned}$$

Now, inverting the matrix A, it is possible to eliminate the unknown flux in the two last equation of (8) and solve a reduced system.

Connection to the finite volume method

In the last section we simplified our problem by eliminating the unknown flux. Using a special quadrature rule to integrate the bilinear form $a(\mathbf{q}, \chi)$ in (7) we end up in a problem with one unknown per element, so we get a system of equations like for a cell-centered finite volume method.

To do so we consider $K^{-1}\mu$ as a scalar and constant over the whole domain. The triangulation fulfils a strict Delaunay property (the sum of angles opposite of an edge e_i is strictly smaller than π).

Baranger [**5**] proposed the following quadrature rule on elements:

$$\int_T \mathbf{p}_h \mathbf{q}_h dx = \frac{1}{2} \sum_{i=1}^{3} c_i \phi_{e_i}(\mathbf{p}_h) \phi_{e_i}(\mathbf{q}_h) \tag{12}$$

with $c_i = \cot(\theta_i)$ and θ_i denotes the angle opposite to the edge e_i, $\phi_{e_i}(\mathbf{p}_h) = \int_{e_i} \mathbf{p}_h \cdot \mathbf{n}\, ds$ is the flux of $\mathbf{p}_h$ through edge e_i. (12) is exact for $\mathbf{p}_h$ and $\mathbf{q}_h$ piecewise constant functions.

For $\mathbf{q}_h \in RT_0$, the value $\mathbf{q}_h \cdot \mathbf{n}$ is constant along the edge e_i. So, for $\mathbf{p}_h, \mathbf{q}_h \in RT_0$ the integral

$$\int_T \mathbf{p}_h \mathbf{q}_h \, dx$$

is approximated by

$$\frac{1}{2} \sum_{i=1}^{3} c_i |e_i|^2 p_i q_i,$$

where p_i, q_i are the degrees of freedom of $\mathbf{p}_h, \mathbf{q}_h$ and $|e_i|$ is the length of the edge e_i.

We use this idea to compute the integral over T in (7) for the test function $\boldsymbol{\chi}_i \in \hat{V}_h$ with

$$\int_{e_j} \boldsymbol{\chi}_i(x) \cdot \mathbf{n} \, ds = \delta_{ij}.$$

So supp $(\boldsymbol{\chi}_i)$ consists of two triangles T and T', see Figure 2.

$$\begin{aligned} a(\mathbf{q}_h, \boldsymbol{\chi}_h) &= \frac{1}{2} K^{-1} \mu (c_i + c_i') \phi_{e_i}(\mathbf{q}_h) \phi_{e_i}(\boldsymbol{\chi}_h) \\ &= \frac{1}{2} K^{-1} \mu (c_i + c_i') q_i |e_i|^2. \end{aligned}$$

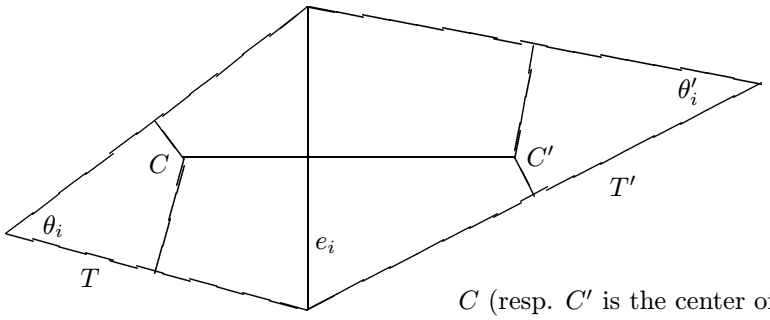

C (resp. C' is the center of the circumscribed circle to T (resp. T'))

Figure 2.

For piecewise constant p, $b(p, \chi)$ is integrated exactly. For such test function we get

$$b(p_h, \boldsymbol{\chi}_h) = p_T - p_{T'}.$$

The integral $(\rho_h \mathbf{g}, \boldsymbol{\chi}_h)$ is approximated by the same quadrature rule (12). It follows that

$$(\rho_h \mathbf{g}, \boldsymbol{\chi}_h) = \frac{1}{2} (c_i + c_i') \rho_{e_i} \mathbf{g} \cdot \mathbf{n}_{e_i} |e_i|^2$$

where ρ_{e_i} is an approximation of ρ on the edge e_i.

By the sine theorem, it follows for D_i, the distance between C and C':

$$\overline{CC'} = \frac{c_i + c_i'}{2}|e_i|\mathbf{n}_i$$
$$D_i = \frac{1}{2}|c_i + c_i^i||e_i|$$

Because of the strict Delaunay property for T, T', it follows:

$$c_i + c_i' > 0\,.$$

An extension to non-Delaunay triangulations is given in ([**5**]).

So, a discrete form of Darcy's law reads as:

$$\begin{aligned}\phi_{e_i}(\mathbf{q}_h) &= q_i|e_i| \\ &= -\frac{K}{\mu}\left\{\frac{p_{T'} - p_T}{D_i}|e_i| - \rho_{e_i}\mathbf{g}\cdot\mathbf{n}_{e_i}|e_i|\right\}.\end{aligned} \tag{13}$$

With the quadrature rule (4) and with Green's formula the second equation in (7) is given by:

$$|T_i|\phi_i\partial_t\rho_{hi} + \sum_{j=1}^{3}\rho_{e_j}\phi_{e_j}(\mathbf{q}_h) = |T_i|\tilde{Q}. \tag{14}$$

Now with (13) it is possible to eliminate the flux $\phi_{e_j}(\mathbf{q}_h)$ in (14) and we get the same discretization as for the well known cell-centered finite volume method.

5. Estimation of the Spatial Error

In order to derive a posteriori error estimates, we consider variational formulations of the continuous and the discrete system. In this section we consider the case $\mathcal{K} \equiv 1$, i.e. without any upwind term, but generalizations to upwind situations are possible.

Multiplying (1) and (2) by functions $r, s \in W_0 \subset W^l_{q'}(\Omega)$, respectively, where q' is conjugate to q from the solution space, and setting $\mathbf{u} := (c, p)$ and $\mathbf{V} := (r, s)$, with $\mathbf{V} \in \mathbf{W}_0 := W_0 \times W_0$, we get a variational formulation, assuming no flow boundary conditions for simplicity both for the fluid and the mass flow or homogeneous Dirichlet conditions by using the following forms:

$$a(\mathbf{u}, \mathbf{V}) := (\rho D\nabla c - \mathbf{q}\rho c, \nabla r) + \Big(\frac{\rho}{\mu}K\nabla p, \nabla s\Big),$$
$$b(\mathbf{u}, \mathbf{V}) := (\Phi\rho c, r) + (\Phi\rho, s),$$
$$\langle \mathbf{f}(\mathbf{u}), \mathbf{V}\rangle := (Q, r) + (\tilde{Q}, s) + \Big(\frac{\rho^2}{\mu}K\mathbf{g}, \nabla s\Big).$$

The variational formulation of the problem (1)–(2) reads as follows:

Find $\mathbf{u}(t) \in \mathbf{V}_0$, $t \in (0,T)$, such that it holds

$$\begin{aligned} \frac{\partial}{\partial t} b(\mathbf{u},\mathbf{V}) + a(\mathbf{u},\mathbf{V}) &= \langle \mathbf{f}(\mathbf{u}),\mathbf{V}\rangle \qquad \forall \mathbf{V} \in \mathbf{W}_0, \\ c(0) &= c_0. \end{aligned} \tag{15}$$

We get the discrete variational form of (6)–(5) by multiplying the equations by $\mathbf{V}_h(x_i)$, with $\mathbf{V}_h := \binom{r_h}{s_h}$, $\mathbf{V}_h \in \mathbf{W}_h := W_h \times W_h$ and summing over all finite volumes. Here $W_h \subset W_0$ and consists of continuous functions.

We set:

$$\begin{aligned} a_h(\mathbf{u}_h,\mathbf{V}_h) &:= \sum_{i=1}^{I} r_{hi} \sum_{j,e} \mathbf{n}_{ij}^e \cdot (\mathbf{q}_{ij}^e \frac{\rho_{ij}^e}{2}(c_i + c_j) - \rho_{ij}^e D_{ij}^e \nabla c_{ij}^e)|\Gamma_{ij}^e| \\ &\quad - \sum_{i=1}^{I} s_{hi} \sum_{j,e} \mathbf{n}_{ij}^e \cdot \Big(\frac{\rho_{ij}^e}{\mu_{ij}^e} K_{ij}^e \nabla p_{ij}^e\Big)|\Gamma_{ij}^e|, \\ b_h(\mathbf{u}_h,\mathbf{V}_h) &:= (\Phi\rho_h c_h, r_h)_l + (\Phi\rho_h, s_h)_l\,, \\ \langle \mathbf{f}_h(\mathbf{u}_h),\mathbf{V}_h\rangle &:= (Q, r_h)_l + (\tilde{Q}, s_h)_l - \sum_{i=1}^{I} s_{hi} \sum_{j,e} \mathbf{n}_{ij}^e \cdot \Big(\frac{(\rho_{ij}^e)^2}{\mu_{ij}^e} K_{ij}^e \mathbf{g}\Big)|\Gamma_{ij}^e|, \end{aligned}$$

where the discrete inner product is defined by

$$(w_h, z_h)_l := \sum_{i=1}^{I} w_{hi} z_{hi} |\Omega_i|. \tag{16}$$

Here q_{ij}^e is the discrete form of (3) as discussed in Section 3.

We remember that for the indices we have $j \in \Lambda_i$ where Λ_i is defined to be the set of indices of all neighbouring nodes x_j to x_i; and $e \in \Lambda_{ij}$, where Λ_{ij} denotes the set of indices e of all elements which contain the nodes x_i and x_j. So we finally arrive at the following discrete problem:

Find $\mathbf{u}_h(t) \in \mathbf{V}_h$, $t \in (0,T)$, such that it holds:

$$\begin{aligned} \frac{\partial}{\partial t} b_h(\mathbf{u}_h,\mathbf{V}_h) + a_h(\mathbf{u}_h,\mathbf{V}_h) &= \langle \mathbf{f}_h(\mathbf{u}_h),\mathbf{V}_h\rangle \qquad \forall \mathbf{V}_h \in \mathbf{W}_h, \\ c_h(0) &= c_{0h}. \end{aligned} \tag{17}$$

The appearing nonlinear variational form is not well investigated. For the sake of simplicity we consider a problem like (17), which fulfill the following assumption:

A1. *There exists* $m_0 > 0$ *such that* $\mathbf{V}, \mathbf{u} \in \mathbf{V}_0$

$$m_0 \|\mathbf{u} - \mathbf{V}\|_{\mathbf{V}_0} \leq \sup_{\mathbf{W} \in \mathbf{W}_0} \frac{a(\mathbf{u}, \mathbf{W}) - a(\mathbf{V}, \mathbf{W})}{\|\mathbf{W}\|_{\mathbf{W}_0}}.$$

A more realistic assumption is formulated in [**2**]. It needs some additional properties of the asymptotic behaviour of the numerical solution, but the demands on the bivariate form are weaker. Besides we need some additional properties about the approximation behaviour of the partition and the chosen subspaces V_h and some properties of the grid.

For the development of indicators for grid adaption we follow the ideas of Bieterman and Babuška [**7**], [**8**] and Angermann [**2**]. We separate the elliptic error by considering an auxiliary problem. Angermann generalized the basic techniques of a posteriori error estimation devised by Babuška and Rheinboldt [**4**] for nonlinear equations. The arising local auxiliary problems are estimated further in this work for getting easily computable quantities.

To define the auxiliary stationary problem, we introduce the notation

$$\langle \tilde{\mathbf{f}}, \mathbf{V} \rangle := \langle \mathbf{f}(\mathbf{u}_h), \mathbf{V} \rangle - \frac{\partial}{\partial t} b(\mathbf{u}_h, \mathbf{V})$$

and get as a new problem

$$a(\tilde{\mathbf{u}}, \mathbf{V}) = \langle \tilde{\mathbf{f}}, \mathbf{V} \rangle \qquad \forall \mathbf{V} \in \mathbf{W}_0. \tag{18}$$

For the error estimation we use

$$\|\mathbf{u} - \mathbf{u}_h\|_{\mathbf{V}_0} \leq \|\mathbf{u} - \tilde{\mathbf{u}}\|_{\mathbf{V}_0} + \|\tilde{\mathbf{u}} - \mathbf{u}_h\|_{\mathbf{V}_0}. \tag{19}$$

Using the assumption **A1** we get

$$\|\tilde{\mathbf{u}} - \mathbf{u}_h\|_{\mathbf{V}_0} \leq \frac{1}{m_0} \sup_{\mathbf{V} \in \mathbf{W}_0} \frac{a(\tilde{\mathbf{u}}, \mathbf{V}) - a(\mathbf{u}_h, \mathbf{V})}{\|\mathbf{V}\|_{\mathbf{W}_0}}.$$

With arbitrary $\mathbf{V}_h \in \mathbf{V}_h$ we get

$$a(\tilde{\mathbf{u}}, \mathbf{V}) - a(\mathbf{u}_h, \mathbf{V}) = a(\tilde{\mathbf{u}}, \mathbf{V} - \mathbf{V}_h) - a(\mathbf{u}_h, \mathbf{V} - \mathbf{V}_h) + a(\tilde{\mathbf{u}}, \mathbf{V}_h) - a(\mathbf{u}_h, \mathbf{V}_h).$$

Omitting the details, we finally obtain for the first term the relation

$$\frac{1}{m_0} \sup_{\mathbf{V} \in \mathbf{W}_0} \frac{a(\tilde{\mathbf{u}}, \mathbf{V} - \mathbf{V}_h) - a(\mathbf{u}_h, \mathbf{V} - \mathbf{V}_h)}{\|\mathbf{V}\|_{\mathbf{W}_0}} \leq C_0 \eta_0$$

with $\eta_0^q = \sum_{i=1}^N \eta_{0i}^q$ and $\eta_{0i} = \sum_{l=0}^3 C_l \tilde{\eta}_{0i}^{(l)}$, where $C_l > 0$ are certain constants and

$$\tilde{\eta}_{0i}^{(0)} := \Big\{ \sum_{\substack{\tau:\tau\not\subset\partial\Omega \\ \tau\cap\Omega_i\neq\emptyset}} h_\tau^{q/2} \int_\tau [\mathbf{n}_\tau \cdot (\mathbf{q}_h\rho_h c_h - \rho_h D_h \nabla c_h)]_\tau^q \, dx \Big\}^{1/q},$$

$$\tilde{\eta}_{0i}^{(1)} := \Big\{ \sum_{\substack{\tau:\tau\not\subset\partial\Omega \\ \tau\cap\Omega_i\neq\emptyset}} h_\tau^{q/2} \int_\tau [\rho_h \mathbf{n}_\tau \cdot \mathbf{q}_h]_\tau^q \, dx \Big\}^{1/q},$$

$$\tilde{\eta}_{0i}^{(2)} := h_i \Big\{ \sum_{T:T\cap\Omega_i\neq\emptyset} \|Q - \Phi\frac{\partial \rho_h c_h}{\partial t} - \nabla\cdot(\mathbf{q}_h\rho_h c_h - \rho_h D_h\nabla c_h)\|_{L^q(T)}^q \Big\}^{1/q},$$

$$\tilde{\eta}_{0i}^{(3)} := h_i \Big\{ \sum_{T:T\cap\Omega_i\neq\emptyset} \|\tilde{Q} - \Phi\frac{\partial \rho_h}{\partial t} - \nabla\cdot(\rho_h\mathbf{q}_h)\|_{L^q(T)}^q \Big\}^{1/q}.$$

Here τ denotes an edge of an element T from $\mathcal{T}$ with length h_τ, $h_i := \max_{T:T\cap\Omega_i\neq\emptyset}\Big\{\max_{\tau\subset\partial T} h_\tau\Big\}$ is a characteristic local mesh parameter and $[\cdot]_\tau$ is the absolute value of the jump across the edge τ (with normal direction $\mathbf{n}_\tau$, where $\mathbf{n}_\tau$ is the outer normal vector at τ w.r.t. T).

To treat the second term, we start from the following decomposition:

$$\begin{aligned}
a(\tilde{\mathbf{u}}, \mathbf{V}_h) - a(\mathbf{u}_h, \mathbf{V}_h) = {} & \sum_{i=1}^N \int_{\Omega_i} \Big[Q - Q_i - \Phi\frac{\partial\rho_h c_h}{\partial t} + \Phi_i \frac{\partial \rho_{hi} c_{hi}}{\partial t}\Big] r_{hi}\, dx \\
& + \sum_{i=1}^N \int_{\Omega_i} \Big[\tilde{Q} - \tilde{Q}_i - \Phi\frac{\partial\rho_h}{\partial t} + \Phi_i\frac{\partial\rho_{hi}}{\partial t}\Big] s_{hi}\, dx \\
& - \sum_{i=1}^N r_{hi}\Big[\int_{\Omega_i} \nabla\cdot(\mathbf{q}_h\rho_h c_h - \rho_h D_h\nabla c_h)\, dx \\
& - \sum_{j,e} \mathbf{n}_{ij}^e \cdot (\mathbf{q}_{h\Gamma_{ij}^e}\rho_{ij}^e c_{ij}^e - \rho_{ij}^e D_{ij}^e \nabla c_{ij}^e)|\Gamma_{ij}^e|\Big] \\
& - \sum_{i=1}^N s_{hi}\Big[\int_{\Omega_i} \nabla\cdot(\rho_h\mathbf{q}_h)\ dx - \sum_{j,e} \rho_{ij}^e \mathbf{n}_{ij}^e \cdot \mathbf{q}_{ij}^e |\Gamma_{ij}^e|\Big] \\
& + \sum_{i=1}^N \int_{\Omega_i} \Big[Q - \Phi\frac{\partial\rho_h c_h}{\partial t} - \nabla\cdot(\mathbf{q}_h\rho_h c_h - \rho_h D_h\nabla c_h)\Big](r_h - r_{hi})\, dx \\
& + \sum_{i=1}^N \int_{\Omega_i} \Big[\tilde{Q} - \Phi\frac{\partial\rho_h}{\partial t} - \nabla\cdot(\rho_h\mathbf{q}_h)\Big](s_h - s_{hi})\, dx
\end{aligned}$$

$$+\sum_{T\in\mathcal{T}}\sum_{\tau\subset\partial T}\int_\tau \mathbf{n}_\tau\cdot(\mathbf{q}_h\rho_h c_h-\rho_h D_h\nabla c_h)r_h\,dx$$
$$+\sum_{T\in\mathcal{T}}\sum_{\tau\subset\partial T}\int_\tau \rho_h\mathbf{n}_\tau\cdot\mathbf{q}_h s_h\,dx\,.$$

The first four terms are estimated straightforward via Hölder's inequality and by making use of the equivalence of the norm $\left\{\sum_{i=1}^I |w_{hi}|^{q'}|\Omega_i|\right\}^{1/q'}$ (cf. (16)) on the components of $\mathbf{V}_h$ with the $L^{q'}(\Omega)$-norm. The estimates of the fifth and the sixth term are in fact estimates of the lumping error. The last two terms are estimated by means of scaled trace inequalities.

For the other term in (19) we assume, that $\exists\delta\in(0,T)\ \exists C_T>0\ \exists\kappa>0$ $\forall t\in(\delta,T)$:

$$\|\mathbf{u}-\tilde{\mathbf{u}}\|_{\mathbf{V}_0}\le C_T h^\kappa\eta_0$$

Collecting the components of the estimators and putting similar terms together, we finally obtain the estimate

$$\|\mathbf{u}(t)-\mathbf{u}_h(t)\|_{V_0}\le\frac{1}{m_0}\sum_{l=0}^{7}C_l\tilde{\eta}_l\qquad\text{with}\quad\tilde{\eta}_l^q:=\sum_{i=1}^{N}\tilde{\eta}_{li}^q$$

and

$$\tilde{\eta}_{0i}:=|\Omega_i|^{-1/q'}\left|\int_{\Omega_i}\left[Q-Q_i-\Phi\frac{\partial\rho_h c_h}{\partial t}+\Phi_i\frac{\partial\rho_{hi}c_{hi}}{\partial t}\right]dx\right|,$$
$$\tilde{\eta}_{1i}:=|\Omega_i|^{-1/q'}\left|\int_{\Omega_i}\left[\tilde{Q}-\tilde{Q}_i-\Phi\frac{\partial\rho_h}{\partial t}+\Phi_i\frac{\partial\rho_{hi}}{\partial t}\right]dx\right|,$$
$$\tilde{\eta}_{2i}:=|\Omega_i|^{-1/q'}\Big|\int_{\Omega_i}\nabla\cdot(\mathbf{q}_h\rho_h c_h-\rho_h D_h\nabla c_h)\,dx$$
$$-\sum_{j,e}\mathbf{n}_{ij}^e\cdot(\mathbf{q}_{ij}^e\frac{\rho_{ij}^e}{2}(c_i+c_j)-\rho_{ij}^e D_{ij}^e\nabla c_{ij}^e)|\Gamma_{ij}^e|\Big|,$$
$$\tilde{\eta}_{3i}:=|\Omega_i|^{-1/q'}\left|\int_{\Omega_i}\nabla\cdot(\rho_h\mathbf{q}_h)\,dx-\sum_{j,e}\rho_{ij}^e\mathbf{n}_{ij}^e\cdot\mathbf{q}_{ij}^e|\Gamma_{ij}^e|\right|,$$
$$\tilde{\eta}_{4i}:=\Big\{\sum_{\substack{\tau:\tau\notin\partial\Omega\\ \tau\cap\Omega_i\neq\emptyset}}h_\tau^{q/2}\int_\tau[\mathbf{n}_\tau\cdot(\mathbf{q}_h\rho_h c_h-\rho_h D_h\nabla c_h)]_\tau^q\,dx\Big\}^{1/q},$$
$$\tilde{\eta}_{5i}:=\Big\{\sum_{\substack{\tau:\tau\notin\partial\Omega\\ \tau\cap\Omega_i\neq\emptyset}}h_\tau^{q/2}\int_\tau[\rho_h\mathbf{n}_\tau\cdot\mathbf{q}_h]_\tau^q\,dx\Big\}^{1/q},$$
$$\tilde{\eta}_{6i}:=h_i\Big\{\sum_{T:T\cap\Omega_i\neq\emptyset}\|Q-\Phi\frac{\partial\rho_h c_h}{\partial t}-\nabla\cdot(\mathbf{q}_h\rho_h c_h-\rho_h D_h\nabla c_h)\|_{L^q(T)}^q\Big\}^{1/q},$$

$$\tilde{\eta}_{7i} := h_i \Big\{ \sum_{T:T\cap\Omega_i\neq\emptyset} \|\tilde{Q} - \Phi \frac{\partial \rho_h}{\partial t} - \nabla\cdot(\rho_h \mathbf{q}_h)\|^q_{L^q(T)} \Big\}^{1/q}.$$

In general, the constants $C_0, \ldots, C_7$ depend on global parameters associated with the bivariate forms $a, a_h, b, b_h, (\cdot,\cdot)$ and with the family of partitions of Ω (cf. also [**1**] for the situation in the case of a linear convection-diffusion problem). For the numerical experiments we take $q = 2$.

6. Adaptive Algorithm and Numerical Experiments

Two kinds of numerical experiments were done. First we consider the adaptive algorithm for the finite volume discretization of flow and transport equation. The main attention is payed to the behaviour of the adaptive procedure. In the second part of experiments we compare the finite volume discretization of the flow equation with the mixed finite element discretization.

We restrict ourselves to 2-d problems. The adaptive procedure for mesh control utilizes the error indicators which have been developed in the previous section 5. Here the basic strategy is to get an equidistribution of the following local indicators:

$$\eta_i := \sum_{l=0}^{7} \frac{\tilde{\eta}_{li}}{\tilde{\eta}_l}, \quad i = 1, \ldots, N\,.$$

In this way we guarantee that all indicators are dimension-free and have an equal influence on the new grid. This representation of indicators is supported by experiments which show that the results are not very sensitive w.r.t. a moderate variation of the weighting factors.

In order to be able to start from a rather coarse initial grid, the first step of the algorithm is performed by means of a re-starting procedure, i.e. after an evaluation of the indicators corresponding to the actual spatial mesh, it is decided whether the second time step has to be carried out or the mesh has to be refined and then the first time step is to be repeated.

All further time steps are passed through only once. During the computations the adaptive algorithm is used only eventually, i.e. the grid is kept fixed for a number of time steps.

In the computations the software package UG from the University of Stuttgart is used. The arising nonlinear system is linearized via Newton's method and the linear equations are solved by a multigrid method. The size of the time step is chosen by the nonlinear solver of UG. For further information about UG and the built-in solvers see [**6**].

A widely accepted test example is so-called Elder problem. There Ω is a rectangular domain $(0, 600) \times (0, 150)$ in the x-z-plane. The data are: $K \equiv 4.845 \cdot 10^{-13}\, I$ (where I is the identity matrix), $D \equiv 3.565 \cdot 10^{-6}\, I$, $\mu \equiv 10^{-3}$, $\phi \equiv 1/10$,

$Q \equiv \tilde{Q} \equiv 0$, $g = \binom{0}{-9.81}$. The density is of the form $\rho = 1000 + 200\,c$. Furthermore, $c_0 = 0$. The boundary conditions are as follows: $c \equiv 1$ for $z = 150$, $x \in [150, 450]$ and $c \equiv 0$ elsewhere, $\mathbf{n} \cdot \mathbf{q} = 0$ on the whole boundary. Since the pressure is determined up to an additive constant, we additionally require $p = 0$ in the point $\binom{0}{150}$.

As a second example we consider a modification of the Elder problem. Here within the rectangular domain $(0, 600) \times (0, 300)$ we have several subdomains. We have jumps of permeability over the boundaries of the subdomains, particular: $K \equiv 4.845 \cdot 10^{-13}\, I$ in the subdomain Ω_1. $K \equiv 4.845 \cdot 10^{-16}\, I$ elsewhere, for the adaptive procedure, and

$$K = \begin{pmatrix} 4.845 \cdot 10^{-13} & 0 \\ 0 & 4.845 \cdot 10^{-16} \end{pmatrix}$$

for the mixed elements. All other coefficients and the boundary conditions are like in the Elder problem.

6.1 Numericals Results for the Adaptive Algorithm

Because no exact solution is known for the Elder problem, we look for the plausibility of the adaptive procedure. In the Figures 3 and 4 the concentration contour lines and the adaptive grids for the time 1.5 and 3.5 years are shown. The grids consist of 6 234 and 6 910 nodes, respectively. We see that the evolution of

Figure 3. Concentration contours and adaptive grid at $t = 1.5$ years.

Figure 4. Concentration contours and adaptive grid at $t = 3.5$ years.

the grid closely follows the evolution of the concentration profile. The algorithm resolves well the most important areas of the computational problem. The solution is compared with a results on a uniform grid of 16 384 nodes in Figure 5. The qualitative behaviour of the solution is the same with significantly less computational costs for the adaptive procedure. The computational costs of the indicators are comparatively low because no additional boundary value problems are to be solved. For the specific problem, only 10% of the total computing time is spent to compute the estimator and for grid-refinement.

Figure 5. Concentration contours for a uniform grid at $t = 3.8$ years.

For the modified Elder problem we look for the behaviour of the adaptive algorithm near inner boundaries. It is well known in literature [**10**] that the jump of the coefficients at the inner boundaries may cause problems. In Figure 6 the

Figure 6. Velocity field, adaptive grid and concentration contours at $t = 10$ years.

contour lines of the concentration, the velocity field and the adaptive grid are presented for the time 10 years. The grid consists of 16 157 nodes. Like in the Elder problem we notice that the grid follows the contour lines of the concentration. Moreover, at the inner boundaries of the domain the finer grid sizes appear. So the area, where we suppose the most problems in calculation, are of finer grid size.

6.2 Numericals Results for the Mixed Finite Element Method

The purpose of this section is to discuss and to compare the differences between the finite volume method (FV) and the mixed finite element method (MFE).

In FV one obtains a linear approximation of the pressure p. The calculation of the Darcy flux $\mathbf{q}$ with the consistent velocity approximation results in a cellwise constant $\mathbf{q}$. In MFE the pressure p and the velocity is approximated individually. This leads to a piecewise constant pressure in each element (or a non-conform linear pressure in each element [**3**]) and a piecewise linear approximation for velocity in the elements.

This difference becomes clear by the Figures 7 and 8. They show the velocity field for the modified Elder example after the first time step.

Figure 7. Velocity field from FV.

Figure 8. Velocity field from MFE.

Figure 9. Velocity field and concentration from FV.

Figure 10. Velocity field and concentration from MFE.

A further difference between FV and MFE is the mass conservation property. The FV fulfils this property on the finite volumes Ω_i and the MFE on elements. It is easy to see that for the problems with strong discontinuous or anisotropic permeability the results of the MFE are more realistic as for FV on the same grid.

References

1. Angermann L., *An a posteriori estimation for the solution of elliptic boundary value problems by means of upwind fem*, IMA Journal of Numerical Analysis **12** (1992), 201–215.

2. _____, *A posteriori error estimates for approximate solutions of nonlinear equations with weakly stable operators*, Preprint 209, Institut für Angewandte Mathematik, Universität Erlangen-Nürnberg, 1996.

3. Arnold D. N. and Brezzi F., *Mixed and nonconforming finite element methods: Implementation, postprocessing and error estimates*, M^2AN **19**(1) (1985), 7–32.

4. Babuška I. and Rheinboldt W. C., *Error estimates for adaptive finite element computations*, SIAM Journal on Numerical Analysis **15**(4) (1978), 736–754.

5. Baranger J., Maitre J. and Oudin F., *Connection between finite volume and mixed finite element method*, M^2AN **30**(4) (1996), 445–465.

6. Bastian P. and Wittum G., *Adaptive multigrid methods: The UG concept*, Adaptive methods-Algorithms, theory and applications, Proceeding of the Ninth GAMM Seminar, Kiel, January 22.-24. 1993 (W. Hackbusch and G. Wittum, eds.), Vieweg,, Braunschweig-Wiesbaden, 1994, pp. 17–37.

7. Bieterman M. and Babuška I., *The finite element methode for parabolic equations i. a posteriori error estimation*, Numerische Mathematik **40** (1982), 339–371.

8. ———, *The finite element methode for parabolic equations i. a posteriori error estimation and adaptive approach*, Numerische Mathematik **40** (1982), 373–406.

9. Brezzi F. and Fortin M., *Mixed and hybrid finite element methods*, Springer-Verlag, 1991.

10. Durlowsky L., *Accuracy of mixed and control volume finite element approximation to darcy velocity and related quantities*, Water Resources Research **30**(4) (1994), 965–973.

11. Frolkovič P., *Maximum principle and local mass balance for numerical solutions of transport equations coupled with variable density flow*, Acta Mathematica Universitatis Comenianae **LXVII**(1) (1998), 137–157.

12. Knabner P. and Frolkovič P., *Consistent velocity approximations in finite element or volume discretizations of density driven flow in porous media*, Computational Methods in Water Resources XI, Cancun. (A. A. Aldama et. al., ed.), Computational Mechanics Publications. Southampton, 1996, pp. 83–100.

13. Leijnse A., *Three-dimensional modeling of coupled flow and transport in porous media*, PhD thesis, University of Notre Dame, Indiana, 1992.

14. Voss C. I. and Souza W. R., *Variable density flow and solute transport simulation of regional aquifers containing a narrow freshwater-saltwater transition zone*, Water Resources Research **23** (1987), 1851–1866.

P. Knabner, Universität Erlangen-Nürnberg, Institut für Angewandte Mathematik I, Martensstraße 3, D–91058 Erlangen, Germany, *e-mail:* knabner@am.uni-erlangen.de

C. Tapp, Universität Erlangen-Nürnberg, Institut für Angewandte Mathematik I, Martensstraße 3, D–91058 Erlangen, Germany, *e-mail:* tapp@am.uni-erlangen.de

K. Thiele, Universität Erlangen-Nürnberg, Institut für Angewandte Mathematik I, Martensstraße 3, D–91058 Erlangen, Germany, *e-mail:* thiele@am.uni-erlangen.de